FULL PAPER

Mesoporous Silicon-PLGA Composite Microspheres for the Double Controlled Release of Biomolecules for Orthopedic Tissue Engineering

*Dongmei Fan, Enrica De Rosa, Matthew B. Murphy, Yang Peng, Christine A. Smid, Ciro Chiappini, Xuewu Liu, Paul Simmons, Bradley K. Weiner, Mauro Ferrari, and Ennio Tasciotti**

In this study, poly(DL-lactide-co-glycolide)/porous silicon (PLGA/pSi) composite microspheres, synthesized by a solid-in-oil-in-water (S/O/W) emulsion method, are developed for the long-term controlled delivery of biomolecules for orthopedic tissue engineering applications. Confocal and fluorescent microscopy, together with material analysis, show that each composite microsphere contained multiple pSi particles embedded within the PLGA matrix. The release profiles of fluorescein isothiocyanate (FITC)-labeled bovine serum albumin (FITC-BSA), loaded inside the pSi within the PLGA matrix, indicate that both PLGA and pSi contribute to the control of the release rate of the payload. Protein stability studies show that PLGA/pSi composite can protect BSA from degradation during the long term release. We find that during the degradation of the composite material, the presence of the pSi particles neutralizes the acidic pH due to the PLGA degradation by-products, thus minimizing the risk of inducing inflammatory responses in the exposed cells while stimulating the mineralization in osteogenic growth media. Confocal studies show that the cellular uptake of the composite microspheres is avoided, while the fluorescent payload is detectable intracellularly after 7 days of co-incubation. In conclusion, the PLGA/pSi composite microspheres offer an additional level of controlled release and could be ideal candidates as drug delivery vehicles for orthopedic tissue engineering applications.

1. Introduction

Porous silicon (pSi) has been widely used for tissue engineering and drug delivery in virtue of its biodegradable and biocompatible nature.[1–4] As a scaffold, pSi is suitable for directing the growth of neuronal cells[5] and for stimulating mineralization in bone tissue engineering.[6–8] For therapeutic delivery, pSi has been administered orally,[9] intravenously,[10] or injected percutaneously and intraperitonealy in humans for brachytherapy without notable side effects.[11] A wide variety of therapeutic and imaging agents have been successfully loaded into and released from pSi particles including steroids,[12] hormones,[13] proteins,[14] cancer drugs,[15] iron oxide nanoparticles,[16] quantum dots, liposomes[17] and carbon nanotubes[18,19] showing the great versatility of this material as a delivery system. Also, the size and shape as well as the porosity and pore size of the pSi particles can be engineered and tightly controlled during manufacturing in order to provide a material with constant and uniform physical features at the

Dr. D. Fan, Dr. E. De Rosa, Dr. M. B. Murphy, Prof. X. Liu, Prof. E. Tasciotti
Department of Nanomedicine
The Methodist Hospital Research Institute
Houston, TX 77030, USA
E-mail: etasciotti@tmhs.org
Y. Peng
Department of System Biology
The University of Texas
M. D Anderson Cancer Center
7435 Fannin Street, Unit 950, Houston, Texas 77054, USA
C. A. Smid, Dr. C. Chiappini
Department of Biomedical Engineering
The University of Texas at Austin
Austin, TX 78712, USA
Prof. P. Simmons
Center for Stem Cell Research
Institute of Molecular Medicine
The University of Texas Health Science Center at Houston
Houston, TX 77030, USA
B. K. Weiner
Department of Orthopedic Surgery
Weill Cornell Medical College
The Methodist Hospital
Houston Texas, Houston, TX 77030, USA
Prof. M. Ferrari
President and CEO
The Methodist Hospital Research Institute Houston
TX 77030, USA

DOI: 10.1002/adfm.201100403

micro- and nanometer scale and to control degradation time and kinetics as well as biodistribution and bioaccumulation.[20] Additionally, their surface can be functionalized to accommodate various drugs, control cellular uptake, target specific tissues[21] and alter their biodistribution in murine models,[17,22] thus allowing for the accumulation of therapeutic agents at tumor sites,[23] or in reservoirs able to sustain the release of nanoliposomes carrying small interfering RNA (siRNA). [24]

Poly(DL-lactide-co-glycolide) (PLGA), a food and drug administration (FDA) approved biodegradable polymer, has been widely investigated for drug delivery applications due to a number of advantageous features.[25,26] First, its degradation rates can be tailored to obtain controlled delivery of drugs. Secondly, the material properties can be adjusted by changing the lactic acid and glycolic acid ratio or molecular weight. Thirdly, PLGA nanoparticles or microparticles can be formulated in order to load not only small molecules but also proteins and larger payloads.[27–29] However, some issues that remain unsolved include the achievement of a uniform, zero order, sustained, linear release and to prevent the initial burst release typical of most PLGA systems.[30] Additionally, the acidic PLGA degradation by-products decrease the pH of the surrounding environment, which may cause undesired inflammatory responses.[31] Finally, the available fabrication methods for PLGA microparticles are incompatible with water-soluble proteins as they may degrade or denature at the organic/inorganic interface during formulation processes.[32]

In this study, we demonstrated that the addition of pSi particles to PLGA microspheres offers a solution to each one of the aforementioned issues. pSi particles, due to their high surface area and interconnected pores, allow for the storage and protection of large amounts of therapeutic molecules.[33] Additionally, PLGA coating provides a tunable layer to seal pSi pores, slow down pSi degradation, and extend the release of the payload. Orthosilicic acid, the by-product of pSi degradation,[34] can neutralize the acidic pH of the PLGA degradation products thus creating less harsh and more cell friendly conditions in the microenvironment both *in vitro* and *in vivo*.[35] The use of hydrophilic pSi particles increased the hydrophilicity of the PLGA/pSi system and improved cell anchorage while not affecting cell proliferation. When the soluble proteins were efficiently loaded within the pores of the pSi particles, their structural integrity (biostability) was preserved. Furthermore, orthosilicic acid promotes collagen formation and facilitates the deposition of calcium and other minerals, thus stimulating bone formation in orthopedic tissue engineering applications.[36,37]

2. Results and Discussion

2.1. pSi Particles

Quasi-hemispherical shaped pSi shells of 3.2 μm in diameter and 600 nm shell thickness (as shown in **Figure 1**) were fabricated according to established protocols.[18] The average pore size was 20 nm with 51% porosity as determined from the desorption branch of nitrogen adsorption/desorption isotherms (data shown in supporting material). In order to turn the pSi surface from hydrophobic to hydrophilic, the pSi surface was

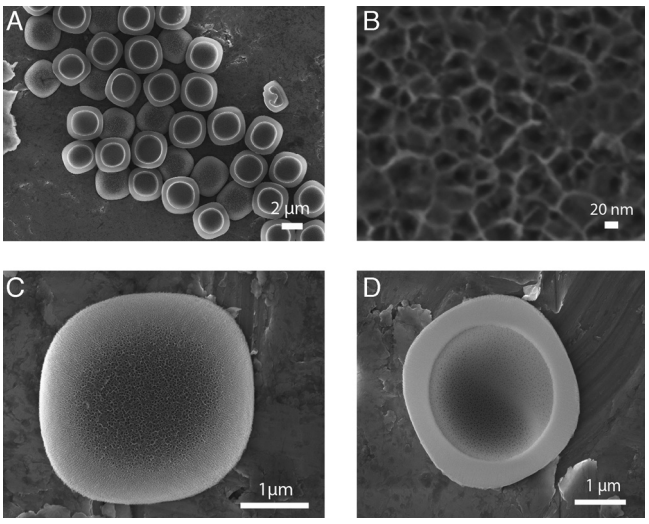

Figure 1. Scanning electron microscopy (SEM) images of pSi particles reveals (A) uniform shape and size of particles, B) the pore structure on the surface of the particles, C) the front, and D) the rear surfaces of the particles.

modified with (3-aminopropyl) triethoxysilane (APTES). Zeta potential analysis showed that the surface charge of the particles after APTES modification had a value of 6.44 mV, while the oxidized pSi surface had a surface charge of −30.39 mV. Once resuspended in IPA, the surface charge of the APTES modified particles showed no notable change for two weeks, thus indicating stable modification of the exposed silicon layer (data shown in the Supporting Information). According to our previous studies, APTES modified pSi particles fully degraded after 18 h in serum.[38]

2.2. PLGA/pSi microsphere Characterization

The overall aspect and the morphology of the microspheres were characterized by optical, confocal, and scanning electron microscopy. **Figure 2**A shows the SEM images of fluorescein isothiocyanate (FITC)-labeled bovine serum albumin (FITC-BSA) loaded microspheres. Figure 2B shows the transmission electron microscopy (TEM) image of the composite material revealing the pSi particles (brown dots, see arrows) embedded in the transparent spherical PLGA particles. These images indicate that the pSi particles had been fully encapsulated in the PLGA spheres. Fluorescent microscopy (Figure 2C) shows the same results. FITC-BSA diffused from pSi particles into the PLGA layer. Figure 2D illustrates the size distribution of the PLGA/pSi microspheres. The microspheres displayed a distribution of sizes ranging from a few microns to approximately 50 μm with an average diameter of 24.5 ± 9.54 μm (145 microspheres were measured).

2.3. PLGA/pSi Microsphere Sorting

PLGA/pSi microspheres prepared with 488-DyLight conjugated pSi particles were characterized before and after centrifugation

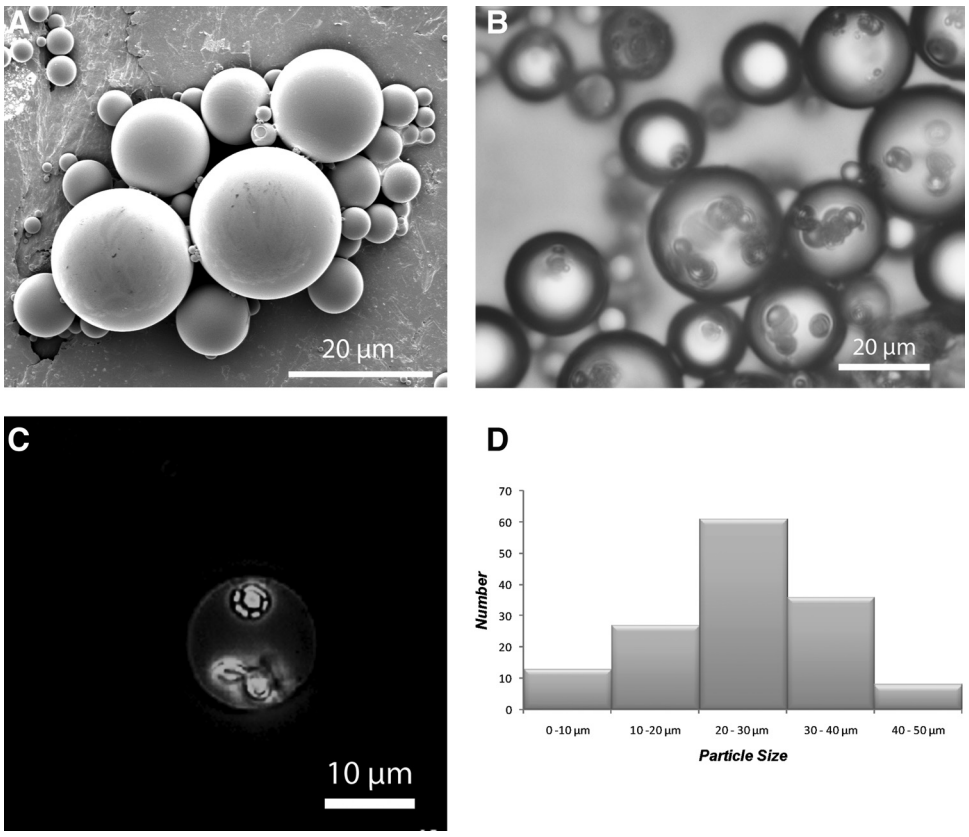

Figure 2. Physical characterization and size distribution of PLGA/pSi microspheres. A) SEM image of presorted microspheres. B) An optical microscopy image shows the presence of pSi particles enclosed in the larger PLGA spheres. C) Fluorescence microscope and (D) The size distribution of PLGA/pSi microspheres displays the uniform product centered around 24.5 µm.

sorting by fluorescence activated cell sorting (FACS) and confocal microscopy (**Figure 3**). FACS data (Figure 3A and 3B) show that the mean fluorescence and hence the percentage of coated particles increases of about one order of magnitude after centrifugation sorting. The coated-fluorescent fraction was initially only the 10% of the sample and after the centrifugation process, it increased to 80%. Moreover the negligible fluorescence of the supernatant reveals the absence of coated particles in it. Its mean fluorescence is two orders of magnitude lower than the original sample and only 1% of it has a comparable fluorescence (Figure 3A and B). Figure 3C shows the fluorescence intensity and distribution of 488-DyLight conjugated pSi particles (light green), unsorted microspheres (blue), sorted microspheres (dark green), and supernatant solution (black).

Confocal images show a mixture of fluorescent and not fluorescent microspheres with polydistributed sizes in the unsorted sample (Figure 3D) and a more uniform particles size after the sorting procedure (Figure 3E), confirming that the sequential centrifugation procedure achieved a good separation of PLGA/pSi microspheres from smaller empty PLGA microspheres.

2.4. Evaluation of FITC-BSA Loading

The surface characteristics significantly affect the ability of FITC-BSA to be loaded into the pores of pSi particles. The BSA had a negative charge at pH 4.7, and APTES modified pSi with a positive charge. The strong electrostatic interaction between the charged amine groups from APTES and acidic moieties of BSA is believed to be the main reason for its high adsorption capacity.[39,40] The amount of FITC-BSA loaded into pSi particles were measured by the mass difference of the loading solutions and the supernatants using a spectrophotometer at 493/518 nm. The loading efficiency of FITC-BSA into pSi particles varied from 53% to 86%, depending on the concentrations of the loading solutions (data shown in supporting material). During the microemulsion step, the loss of the FITC-BSA was approximately 13.24%, 9.84%, and 5.14% from the composites and it inversely correlated with the density of the different PLGA coatings (6%, 10%, and 20%, respectively). This result demonstrated that during synthesis higher concentrations of the coating solutions resulted in lower protein loss.

2.5. In Vitro Release of FITC-BSA

The mass of FITC-BSA released from control and experimental materials was determined by measuring the fluorescence of the collected supernatant using a spectrophotometer at 493/518 nm. The release profiles of FITC-BSA from pSi particles (control), PLGA microspheres (control) and PLGA/pSi microspheres

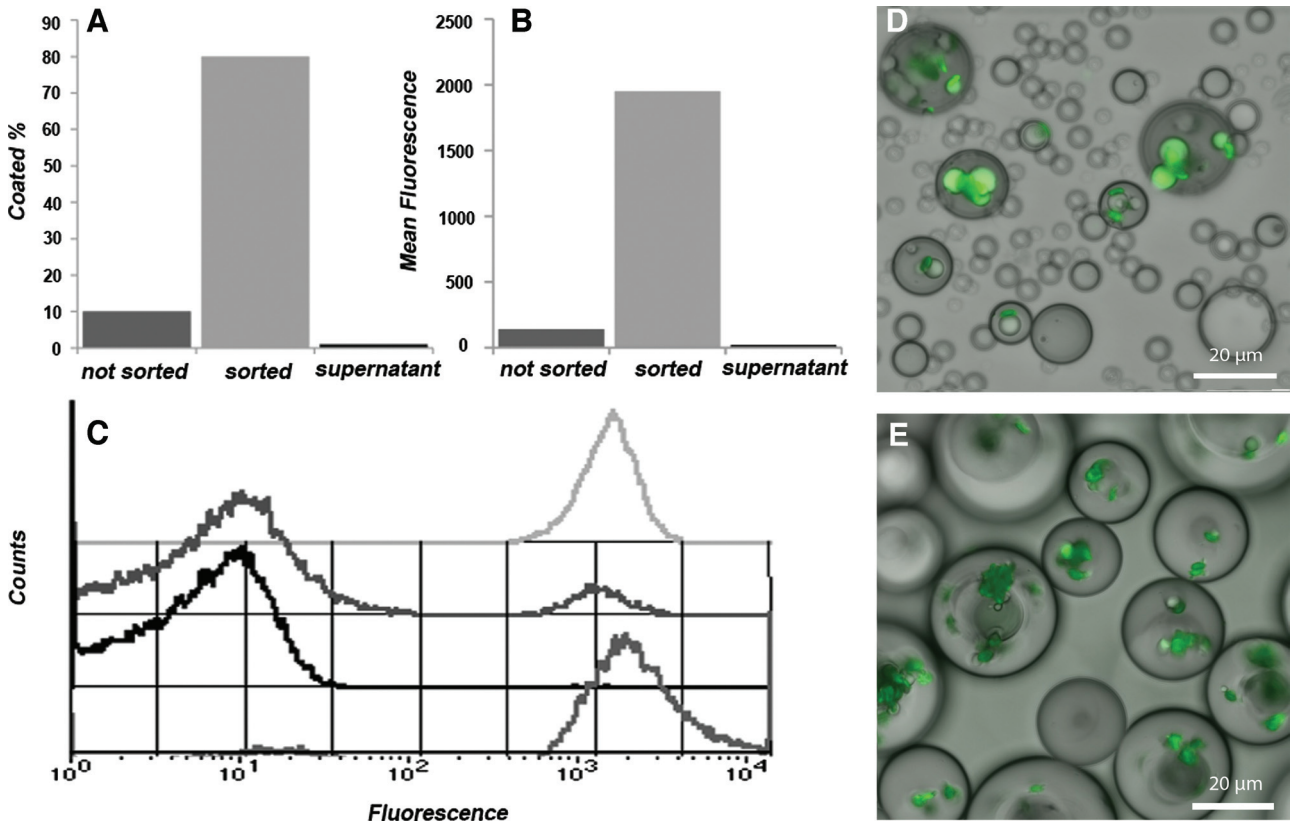

Figure 3. A–C) FACS analysis of unsorted and sorted PLGA/pSi microspheres prepared with 488-DyLight conjugated pSi particles (DyLight-PLGA/pSi microspheres): A) the percent of DyLight-PLGA/pSi microspheres in the non-sorted, sorted microspheres and supernatant; B) the mean fluorescence of the sorted, unsorted microspheres, and the supernatant; C) fluorescence intensity and distribution of 488-DyLight conjugated pSi particles (light green), unsorted microspheres (blue), sorted microspheres (dark green), and supernatant solution (black). D–E) Confocal images of (D) unsorted microspheres (E) sorted microspheres.

are shown in **Figure 4**A. In the case of pSi particles and PLGA microspheres (6%, 10%, and 20%), protein release showed a massive initial burst release which reached the plateau after less than 3 days. On the contrary, PLGA/pSi microspheres released approximately 70% (6% PLGA), 38% (10% PLGA), and 25% (20% PLGA) of the payload at day 3 (Figure 4B). After 2 weeks, the release of FITC-BSA from the composite reached approximately 100% (6% PLGA/pSi), 60% (10% PLGA/pSi), and 40% (20% PLGA/pSi) of the payload as shown in Figure 4C and it continued to be released for other 2 weeks from the higher density PLGA coatings (10% and 20%) (Figure 4D). **Figure 5**A and 5B show that at all time points, PLGA/pSi microparticles showed consistently higher fluorescence when compared to controls. Due to the initial burst release of FITC-BSA during the first 3 days, the fluorescence of PLGA microspheres decreased at fast pace and dropped to its minimum. Conversely, the addition of pSi particles to the PLGA microspheres reduced the FITC-BSA release rate as demonstrated by the higher fluorescence intensity measured throughout the experiment.

All together, the study of the in vitro release of FITC-BSA demonstrated that the PLGA coating played an important role in controlling the release kinetics from the microspheres. A higher concentration of PLGA resulted in a coating layer characterized by higher density and thickness. As a consequence, the diffusion of FITC-BSA through the PLGA layers was slowed down, resulting in lower release rates and more sustained delivery of the payload. Similarly, a thicker layer of PLGA delayed the degradation of the composite microspheres thus additionally slowing down the release of the encapsulated proteins. In all profiles, the two phases observed during protein release were attributed to a minor fraction of the pSi loaded BSA which diffused into the PLGA layer during the microsphere fabrication process and was released earlier than the fraction still loaded into the pores of pSi particles.

2.6. PLGA/pSi Microsphere Degradation

The PLGA/pSi microsphere degradation was studied by monitoring the morphology changes using SEM. **Figure 6** shows the SEM images of three types of PLGA/pSi microspheres (6%, 10%, and 20% PLGA coatings) degradation over six weeks in PBS. At week 1, pores were observed on the surface of all three types of microspheres, showing an early -stage degradation. Pore number and size increased with time and after three weeks, 6% and 10% PLGA/pSi microspheres appeared deformed and partially collapsed. At week 4, more pores appeared on the surface of the

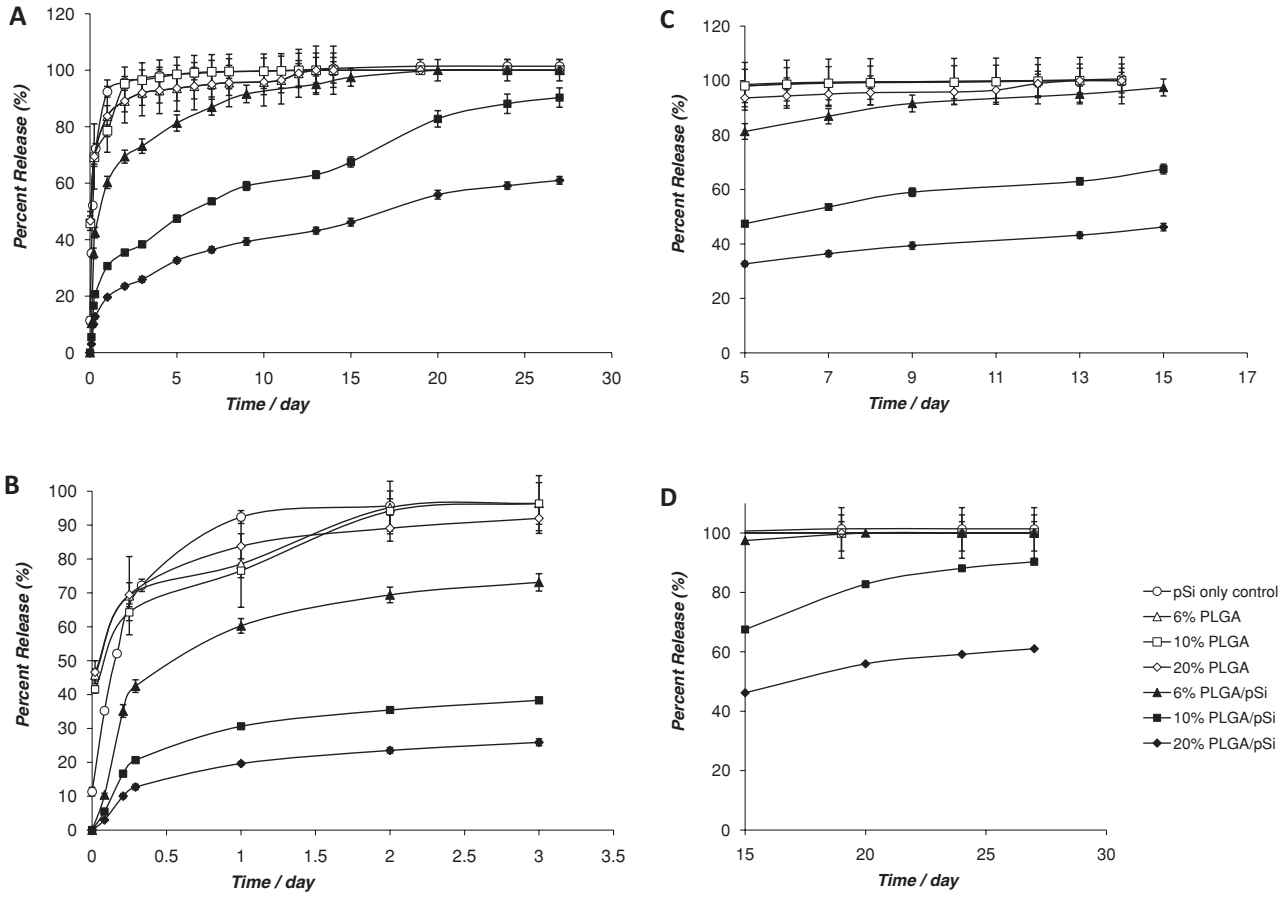

Figure 4. Release profiles of FITC-BSA from various examined PLGA/pSi microsphere formulations. A) Total FITC-BSA released over 27 days, B) first three day release, C) day 5 to 15 release, and D) day 15 to 27 release.

6% PLGA/pSi microspheres, while the surface layers of polymer coatings were peeled off from the 10% and 20% PLGA/pSi microspheres and a porous, sponge-like morphology was observed beneath the surface. At week 6, the 6% PLGA/pSi microspheres completely lost their spherical morphology, while the 10% and 20% PLGA/pSi broke into pieces revealing the inner porous structure of the microsphere.

Figure 7 demonstrates the change of pH in the medium during the degradation of PLGA, pSi, and PLGA/pSi microspheres. The control sample (pSi) kept a constant pH value of approximately 7.2 during the 4-week degradation. PLGA microsphere degradation induced a pH drop at two weeks (Figure 7A). However, when pSi microparticles were introduced to the PLGA microspheres, the pH values recorded were approximately around 7 over the four-week degradation period, and only the microspheres with the thickest coating (20% PLGA) generated acidic conditions after four weeks (Figure 7B). This is due to the fact that the pSi degradation product, orthosilicic acid, buffered the pH at higher values.[41,42] The mass ratio of PLGA to pSi is 5:1 (6% PLGA/pSi), 8:1 (10% PLGA/pSi), and 16:1 (20% PLGA/pSi). The PLGA and pSi particles degrade concurrently, which allows silicic acid to buffer the acidic environment when the acidic products of PLGA are produced. As expected, lower ratios showed higher buffer capacity than the higher ratio.

2.7. BSA Stability Studies

BSA, like all other proteins, is susceptible to hydrolytic degradation in aqueous solutions. These reactions can be catalyzed by acidic molecules, such as the byproducts of PLGA. In order to minimize protein degradation during loading, FITC-BSA was first loaded into pSi microparticles and lyophilized prior to PLGA coating. This step reduces exposure to water during particle preparation and during eventual PLGA degradation. SDS-PAGE of released FITC-BSA and degraded byproducts is exhibited in **Figure 8**. The appearance of bands for degraded proteins is substantially less for PLGA/pSi-released BSA than controls at 7 days. Between 9 and 14 days, a relatively small amount FITC-BSA is released which is insignificant compared to controls and 7 day time points. However, 10% and 20% coating groups show only an intact FITC-BSA band and not small byproducts, indicating that molecules released after one week have not been hydrolytically degraded. This is likely because molecules stored deep within the core of the microparticles are not exposed to any water until the PLGA coating has been sufficiently eroded.

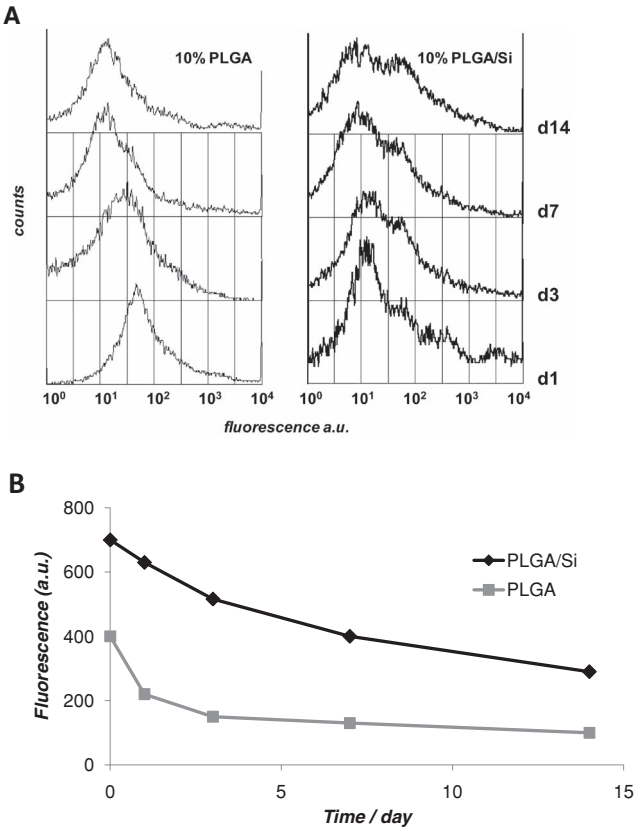

Figure 5. PLGA and PLGA/pSi microspheres analyzed via FACS during in vitro release. A) Histographic overlay of the fluorescence intensity and distribution of control PLGA (left) and PLGA/pSi (right) over two weeks of incubation in PBS. B) Decrease of fluorescence intensity as measured through FACS dropped to a minimum at day 3 in control PLGA. PLGA/pSi showed slow decrease in fluorescence intensity and displayed a three-fold intensity compared to the control at two weeks.

2.8. In Vitro Mineralization Studies

This study has investigated whether the addition of pSi microparticles to PLGA microspheres can enhance the mineral deposition on the microspheres surfaces compared to PLGA microspheres only. After incubation in the osteogenic media for three days, the smooth surface of the PLGA/pSi microspheres was covered with a porous rough layer (**Figure 9**B), while the control PLGA microspheres remained smooth with just minimal crystal deposition on the surface (Figure 9A). After a 21-day incubation, SEM images demonstrate that the surface of PLGA/pSi microspheres was uniformly covered with a layer of mineral deposits (Figure 9D), while the control samples showed negligible signs of calcification under the same conditions at the same time intervals (Figure 9C). This phenomenon was confirmed at higher magnification at SEM (Figure 9E and 9F). These data suggested that the pSi contained in the PLGA microspheres has the ability to stimulate more intense formation of a mineralized layer on the surface. As a confirmation of the formation of the calcium phosphate crystals on the surface of the microspheres, the EDX spectrum showed calcium and phosphorous peaks on the surface layer at day 3 (grey line) and day 14 (black line) (Figure 9G). The mechanism of calcium phosphate deposition is that the polymerized silicic acid acted as heterogeneous nucleation substrate to stabilize the growing of calcium phosphate nuclei. The uniformly coated osteoactive mineral layer will further enhance the osteogenic qualities and the osteoconductive potential of the scaffolds, while still allowing the release of the bioactive molecules due to the inherent porosity of the surface mineralization (see Figure 9F)[37] The PLGA microspheres alone did not show any sign of calcification at day 3 (Figure 9H, grey line), but calcium and phosphate peaks were detected by EDX (Figure 9H, black line) at day 14. However, the calcium and phosphate peak intensity of PLGA microspheres was not as high as that of the PLGA/pSi microspheres. These results demonstrate that the pSi particles have the ability to increase the mineralization and may serve a dual role in bone tissue engineering applications.

2.9. PLGA/pSi Microsphere Internalization by BMSCs

Most growth factors and differentiating stimuli function by binding to cell surface receptors to start active transmembrane signal transduction while the ligand is still in the extracellular space. When growth factors or differentiation stimuli are transported by a nano-sized carrier and the carrier is internalized by the target cells, they are unable to interact with the surface membrane receptors, thus completely losing their function and bioactivity.[43] The intended function of our composite particles is to release bioactive proteins at the site of tissue repair. In these scenarios, macrophages and other inflammatory cells often internalize and degrade nano-sized particles through endocytosis, pinocytosis and phagocytosis.[44,45] In this study, BSA was used as a model growth factor to be delivered by PLGA/pSi microspheres. The PLGA coating around pSi particles prevents internalization due to its size, while providing a hydrophobic barrier to enzymes released by the cells thus protecting for longer times their bioactive payloads. One of the purposes of this study was to determine if the PLGA/pSi microspheres could serve as potential vehicles to successfully deliver growth factors. Confocal microscopy images showed that the 10% PLGA/pSi microspheres (average diameter 24.5 μm) were not internalized by the cells after 0.5 h (**Figure 10**D and 10G), 48 h (Figure 10E and 10H) and 120 h incubation (Figure 10F and 10I). The control images showed accumulation of the uncoated pSi (~3 micron) inside the bone marrow stromal cells within an hour from the beginning of the incubation (Figure 10A, 30 min incubation) and after 48 h (Figure 10B) and 120 h incubation (Figure 10C). No cell death, morphological changes or overall cytotoxicity to BMSCs was observed in vitro during the entire cell culture period, confirming the compatibility of these composite microspheres to cells and surrounding environment. Figure 10J describes the mechanism of action of the pSi particles (right side of the dashed line) versus the PLGA/pSi composite microspheres (left side of the dashed line). While pSi are internalized by BMSCs (Figure 10J2), the PLGA/pSi particles lay on the surface of the BMSCs avoiding cellular uptake (Figure 10J1).

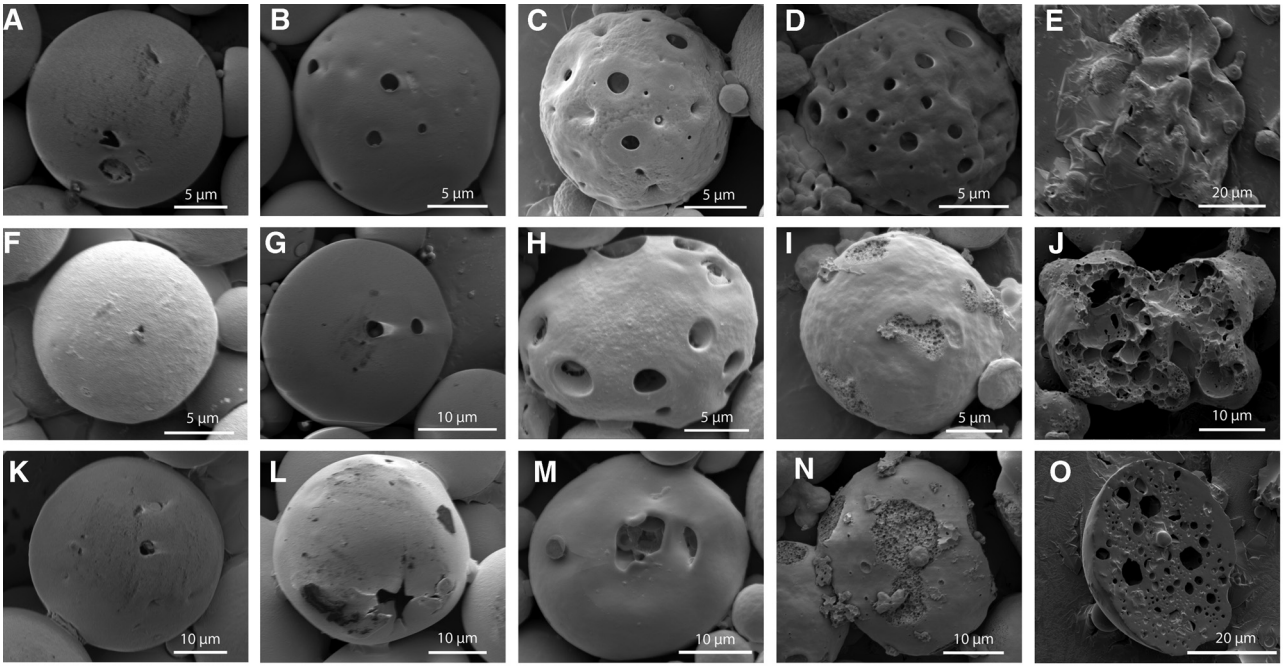

Figure 6. SEM images of PLGA/pSi microsphere degradation over 1, 2, 3, 4, and 6 weeks with 6% coating (A–E), 10% coating (F–J), or 20% coating (K–O).

Furthermore, the internalization of the pSi inside the cell would inevitably result in its entrapment into the lysosomal compartment as shown in Figure 10J2. The acidic environment of lysosomes would denature the growth factors, affect their bioactivity and natural site of action thus resulting in the complete absence of a response to the treatment (Figure 10J4).[46,47] On the contrary, the ability of the PLGA/pSi microspheres to escape internalization results in the double advantage of preventing the exposure of the payload to the hostile lysosomal environment while releasing it in close contact to the external layer of the cellular membrane where most of protein mediated signaling starts. As a consequence of membrane receptor triggering, the signal pathway arrives to the nucleus thus allowing for a change in cell functions (color change in Figure 10J3).

2.10. Cellular Uptake of FITC-BSA Released from PLGA/pSi Microspheres

BSA, like many growth factors, is internalized through receptor-mediated endocytosis (clathrin-mediated endocytosis) and fluid phase endocytosis,[48–53] and was selected as a model protein for the release and cellular uptake studies. As mentioned previously, BSA released in the media activated cell surface receptors to start signal transduction to alter intracellular response and then BSA was internalized by the cells (Figure 10J3). The experiment was performed analogous to in vivo situations, where a burst or single-dose delivery of proteins are quickly diffused away from the delivery site, while PLGA/pSi particles are able to sustain the release of days and weeks. To assess the rate of cellular uptake of the BSA released from the PLGA/pSi microspheres, human umbilical vein endothelial cells (HUVEC) were studied using confocal microscopy after 7 days in culture. HUVEC cells were plated in a transwell without microspheres and incubated with PLGA/pSi in the top chamber (**Figure 11**). Confocal images show an evident cellular uptake of BSA after 7 days of incubation with PLGA/pSi microspheres. Cellular uptake appeared in discrete spots that probably suggesting protein accumulation in subcellular organelles. The control group (BSA initially added in solution) did not show any BSA accumulation in cells after 7 days. This is probably due to intracellular enzymatic degradation of the fluorescent protein. As the media was exchanged every three days, by Day 7 little BSA was available in the supernatent. BSA has a half-life in circulation or serum-based media of 19 to 20 days.[54,55] FITC-BSA (or other model protein) degradation within a cell can occur in as few as 4 h.[56] Fluorescence quantification of the confocal images showed 35 fold increase of the corresponding green fluorescence, while no difference was recorded in the red and blue fluorescence associated to the cytoskeleton (actin) and nucleus (blue) respectively. The findings suggest that FITC-BSA observed within the cells of experimental groups was delivered and internalized within the last 4–2 h prior to measurement, therefore the microparticles are still delivering ample amounts of the proteins at day 7. These results imply that PLGA/pSi microspheres can be used as tunable carriers for releasing bioactive proteins to cells in a controlled and predictable fashion.

3. Conclusions

A novel class of PLGA/pSi microspheres was fabricated by an S/O/W emulsion method by incorporating polymer science with micro-lithography and electrochemical etching.

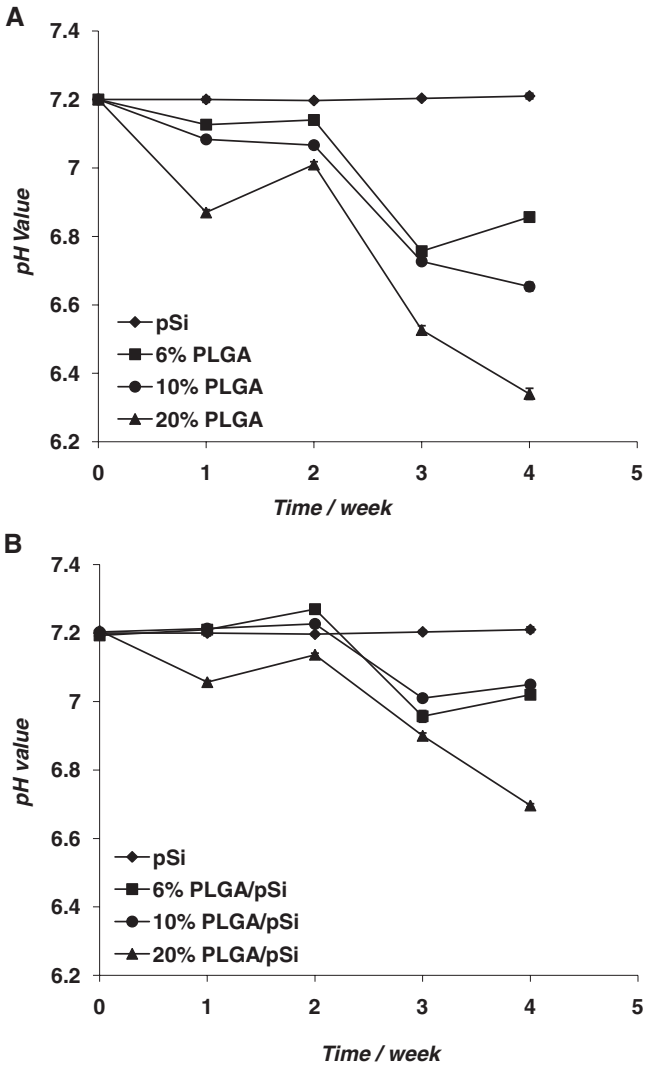

Figure 7. The pH of pSi, PLGA, and PLGA/pSi microsphere degradation byproducts in PBS at 37 °C over 4 weeks for (A) PLGA-only microspheres (control) and (B) PLGA/pSi microspheres.

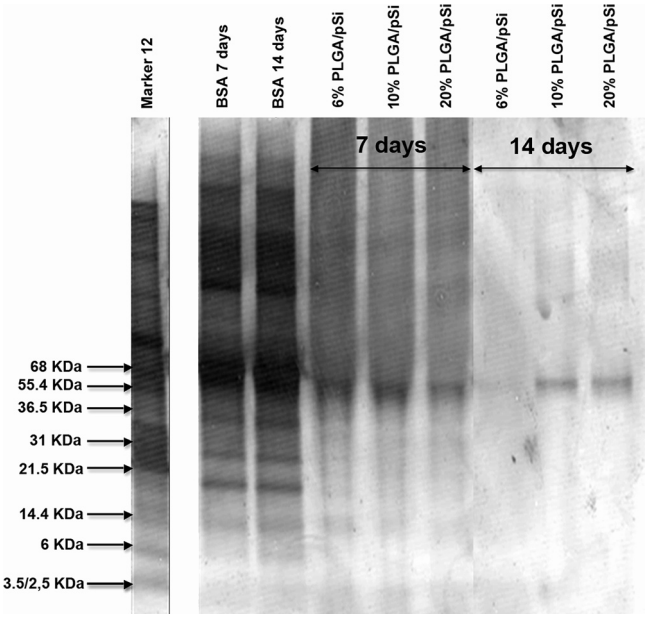

Figure 8. FITC-BSA degradation over two weeks. SPS-PAGE of release products showed BSA (approximately 68 kDa) released from PLGA/pSi microspheres suffered no degradation bands compared to controls (BSA in solution for 7 and 14 days, column 2 and 3, respectively).

This system provided a number of unique advantages over pre-existing drug delivery materials due to its ability to: 1) prevent the burst release of proteins and prolong the delivery over a longer period of time through the tuning of the PLGA coating; 2) counteract the acidification of the environment by PLGA degradation byproducts via buffering with pSi degradation products; 3) preserve protein stability and half-life as the S/O/W method prevents protein degradation during the fabrication process; 4) control cellular internalization and protein accumulation by increasing the particle diameter with PLGA coatings and controlling biomolecular release based on PLGA properties, respectively (PLGA/pSi microspheres cannot be internalized by cells due to their size, which is particularly important for the delivery of growth factors and proteins interacting with extracellular receptors); 5) stimulate mineralization by promoting the deposition of calcium phosphate ions on the particle surface. All together, these findings demonstrate that the PLGA/pSi microspheres show superior properties than traditional PLGA microspheres in terms of prolonged release of molecules and stimulation of mineralization, and represent a promising alternative as drug delivery vehicles for tissue engineering applications. Their use has been already successfully tested in different orthopedic tissue engineering applications in small and large animal models of bone fracture repair (manuscript in preparation).

4. Experimental Section

pSi Particle Fabrication: The pSi particles were fabricated as previously described.[29] Briefly, a layer of silicon nitride (Si_3N_4) (80 nm) was deposited by low pressure chemical vapor deposition on a 4" p-type Si wafer with resistivity <0.005. AZ5209 photoresist (AZ Electronic materials) was spun cast at 5000 R.P.M. for 30 s on the substrate, followed by pre-exposure baking at 90 °C in an oven for 10 min. A pattern consisting of dark field circles (2 μm) with pitch (2 μm) was transferred on the photoresist with a MA/MB6 mask aligner. The pattern was developed for 20 s in MIF 726 developer, and then transferred into the silicon nitride (Si_3N_4) layer and 300 nm into the silicon substrate by two step Reactive Ion Etch (first step: Plasmatherm 790, 25 sccm CF_4, 200 mTorr, 250 W RF, 2 min 20; second step: Oxford Plasmalab 80, 20 sccm SF_6, 100 mTorr, 200 W RF, 4 min). The photoresist was removed from the substrate by an 8 min piranha clean (H_2O_2:H_2SO_4 1:2 v/v). The porous particles were formed by anodic etch in Hydrofluoric acid (HF): ethanol (1:3 v/v) applying a current (0.3 A) for 60 s followed by 3.8 A for 6 s in a custom Teflon etching cell. The Si_3N_4 layer was removed by soaking in HF for 30 min, the substrate was dried and the particles were released in isopropanol (IPA) (Acros) by sonication.

Particle Analysis and Surface Modification of pSi: For oxidation, the dried pSi particles were resuspended in a piranha solution and heated to 110–120 °C for 2 h. The suspension was washed with DI water until the pH was approximately 5.5–6.0. Oxidized pSi particles were suspended in

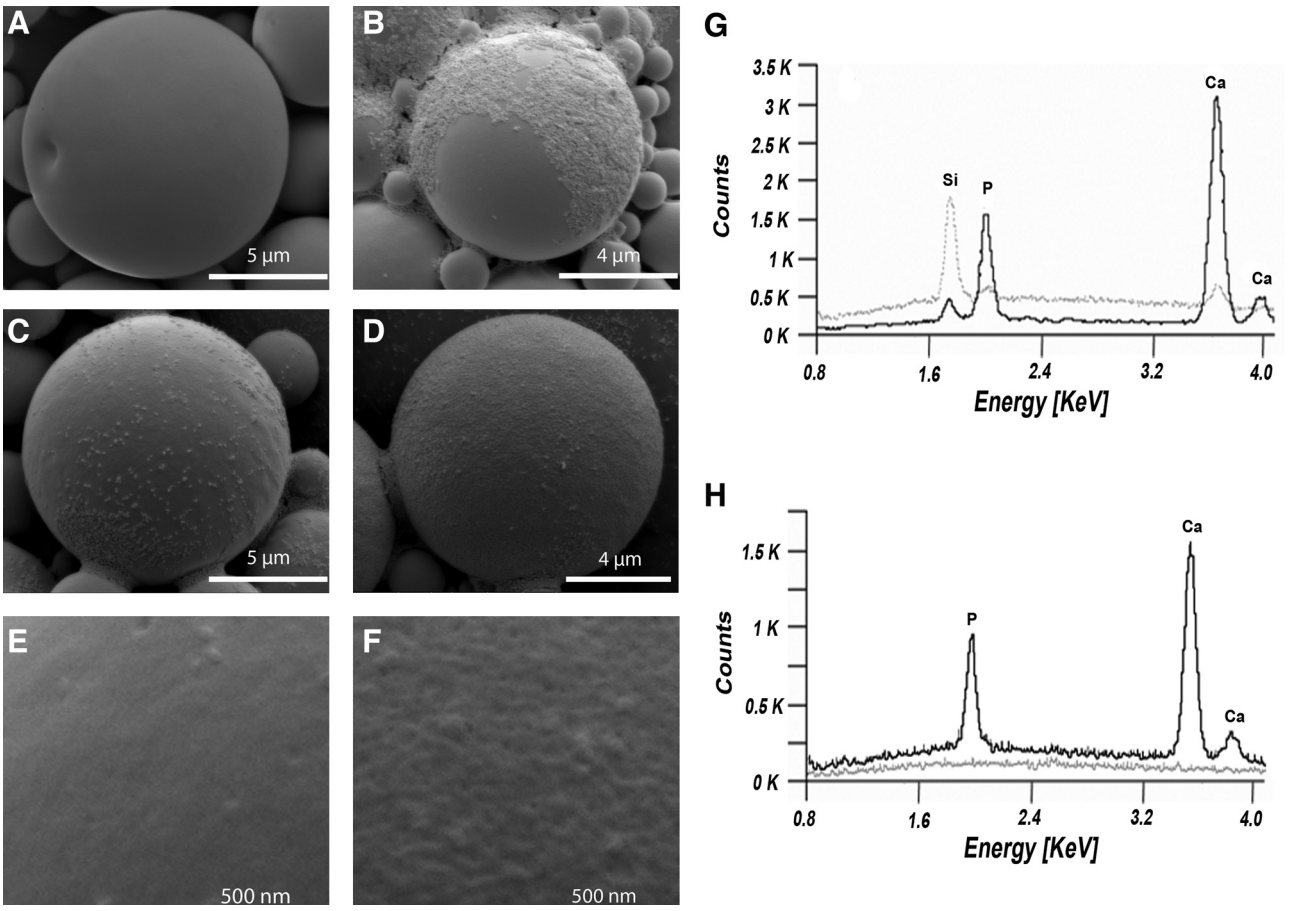

Figure 9. Mineralization on the surface of PLGA/pSi microspheres. SEM images of PLGA (A,C) and PLGA/pSi (B,D) microspheres in osteogenic media after 3 and 21 days. E–F) Results at day 21 at higher magnification. G) EDX spectrum of mineralized PLGA/pSi microspheres on day 3 (gray dot line) and day 14 (black solid line). H) EDX spectrum of PLGA microspheres on day 3 (gray dot line) and day 14 (black solid line).

ISOTON® II Diluent, and counted by a Multisizer 4 Coulter® Particle Counter (Beckman Coulter) with an aperture (20 µm). pSi particles were surface modified with APTES (Sigma–Aldrich) as reported previously.[20] 1×10^8 oxidized particles were suspended in of Millipore water (20 µL). A solution was prepared of 2.0% APTES and 3.0% Millipore water in IPA. This solution (980 µl) was added to the particles and mixed well. This vial was placed to a 35 °C thermomixer set to mix at 1300 rpm for 2 h. After modification, the particles were washed with anhydrous IPA 5 times and moved to a vacuum oven for annealing at 60 °C overnight.

Loading of FITC-BSA into APTES modified pSi particles: FITC-BSA (Sigma–Aldrich) solution (10 mg/mL) was prepared by dissolving FITC-BSA powder in distilled water. 4×10^8 APTES modified particles were immersed into of FITC-BSA solution (200 µL) in an Eppendorf tube. The suspension was incubated on a thermal mixer at 37 °C under agitation for 30 min to allow the adsorption of the protein into the pores of pSi particles. The particles were separated by centrifugation and washed with PBS to remove the FITC-BSA physically absorbed on the surface. The FITC-BSA loaded particles were then lyophilized overnight. The amount of protein absorbed was measured by the difference between the protein concentrations of the stock solution and of the supernatant using SpectraMax M2 spectrophotometer (Molecular Devices).

Preparation of PLGA Particles and PLGA Coated pSi Particles: pSi particles coated with PLGA were prepared by a modified S/O/W emulsion method[57] as shown in **Scheme 1**. Briefly, PLGA (50:50) (Sigma Chemicals Co. St. Louis, MO) was dissolved in dichloromethane (DCM) (Sigma Aldrich) to form 6%, 10%, and 20% w/v PLGA/DCM solution respectively. 8×10^7 FITC-BSA loaded particles were suspended in these solutions (1 mL, 6%, 10%, and 20%) respectively by sonicating the mixture. The organic phase containing the pSi was mixed with of Poly (vinyl alcohol) (PVA) (Fisher Scientific) (3 mL, 2.5% w/v) by vortex mixing and sonication. The mixture was gradually dropped into water (50 mL) containing PVA (0.5% w/v). The resulting suspension was stirred with a magnetic stir bar for 2 h and the DCM was rapidly eliminated by evaporation. The PLGA/pSi microspheres were washed with distilled water. Finally, the product was lyophilized and stored at 4 °C. PLGA particles were prepared in the similar method as PLGA/pSi microsphere fabrication, except that BSA solution instead of BSA loaded pSi particles was mixed with PLGA/DCM.

Characterization of PLGA/pSi Microspheres: The morphology of the microspheres was characterized by optical microscope (Nikon Eclipse TS 100), fluorescent microscope (Nikon Eclipse TE 2000-E), confocal laser microscope (Leica MD 6000), and scanning electron microscope (SEM) (FEI Quanta 400 ESEM FEG). The samples were analyzed by confocal laser microscope at 488 nm to identify the FITC-BSA loaded pSi. The microspheres were also examined by SEM under a voltage of 3 KV. The samples were sputtered with gold (20 nm) by a Plasma Sciences CrC-150 Sputtering System (Torr International, Inc) before SEM analysis.

Sorting Procedure: Several centrifugation steps, optimizing time and rotation rate of each step, were performed to separate the PLGA/pSi microspheres from the empty PLGA microspheres. Separation was carried out by three centrifugation steps of 10 min each at 500, 1200 and 4500 rpm respectively with the Allegra X-22 Centrifuge (Beckman Coulter Inc.). pSi particles conjugated with DyLight 549 NHS-Ester

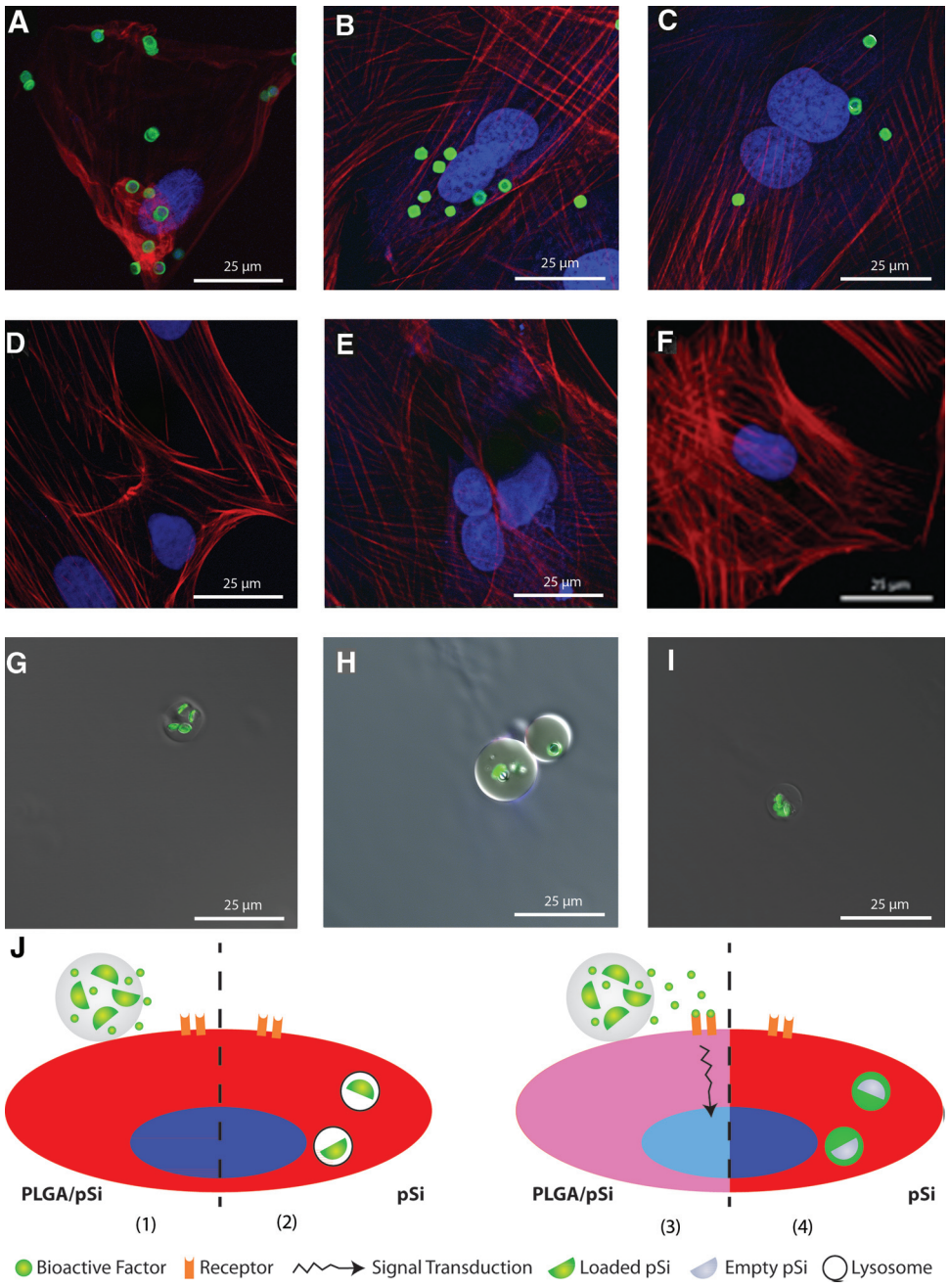

Figure 10. Confocal microscopy images show PLGA/pSi microparticles (loaded with green fluorescent BSA) were not internalized by BMSCs at (D–G) 0 h, (E–H) 48 h, or (F–I) 120 h, while (G) pSi microparticles were internalized by BMSCs in 0.5 h (A), 48 h (B), and 120 h (C). J) A schematic diagram of the mechanism of action of PLGA/pSi microspheres compared to pSi. Following internalization pSi is trapped within lysosomes (J2 and J4) while the PLGA/pSi particles are not endocytosed by BMSC and release their payload outside the cells where it can exert its bioactive function and trigger nuclear changes through the classic mechanism of signal cascade (J3 and J4).

(Thermo Scientific) coated with PLGA were analyzed by FACS (Becton Dickinson, FACSCalibur) before and after sorting procedure to asses sorting efficiency.

Evaluation of FITC-BSA In Vitro Release: 2×10^7 FITC-BSA loaded PLGA/pSi microspheres were dispersed in PBS (1 mL) at 37 °C. At predetermined time intervals, the suspension was centrifuged (4500 rpm; 5 min), and the supernatant (1 mL) was collected, and replaced with fresh PBS (1 mL. The amount of BSA released was determined by analysis of the collected supernatant using a spectrophotometer at 493/518 nm. The suspension was also analyzed by FACS and the samples were prepared by mixing NaCl solution (150 μL) with suspension (5 μL) removed from in vitro release samples.

Degradation Studies: The in vitro degradation of the PLGA/pSi microspheres was investigated by monitoring the surface morphology of the microspheres and the pH of the degradation media. The pH level was monitored using a pH meter (Denver Instrument UB-10), and the surface morphology of the microspheres was examined by SEM.

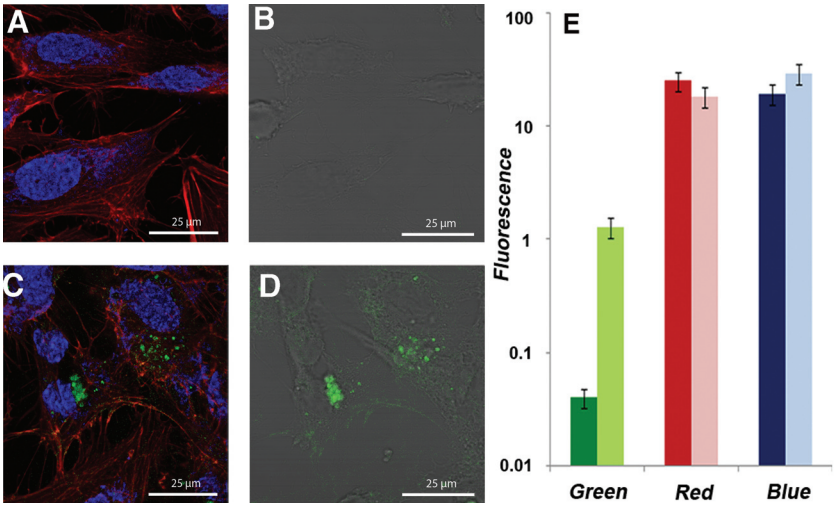

Figure 11. Confocal images of stained HUVEC (green-BSA, red-actine filaments, blue-nuclei) after 7 days in culture (A,B) (control, BSA initially added in solution) or incubated with BSA loaded PLGA/pSi microspheres (C,D), with overlap of all three fluorescent channels (A and C), or bright field and green (B and D). Average fluorescence intensity of the three fluorescent channels (E) related to control HUVEC (dark color bars). HUVEC incubated with PLGA/pSi (light color bars) as measured at the confocal microscope.

BSA Stability Studies: SDS-PAGE gel electrophoresis was performed to determine the hydrolysis of BSA during the FITC-BSA release from PLGA/pSi. Color Silver Staining Kit was used to stain the gel, Mark 12 (Invitrogen) was used as standards. Supernatant (100 μL) released from PLGA/pSi microspheres (6%, 10%, 20%) collected on day 7 and day 14 was filtered by Amicon Ultra-0.5ml centrifugal filter (Millipore Ultracel-3 Membrane, 3 kDa) before SDS-PAGE.

In Vitro Mineralization Studies: The osteogenic media were prepared by base media (α-MEM media) (Invitrogen) containing fetal bovine serum (20%, FBS) (Invitrogen) supplemented with L-glutamine (1%), sodium pyruvate (1%, Invitrogen), penicillin/streptomycin (1%, Invitrogen), and osteogenic supplement. PLGA/PSi microspheres were immersed in osteogenic growth medium. After 3, 8 and 21 day incubation, the specimens were washed carefully with DI water, and dried under vacuum overnight before characterization. PLGA microspheres were used as control. The samples were analyzed by SEM coupled with energy dispersive X-ray (EDX) for mineralization studies.

In Vitro Internalization Studies: 6500 BMSCs were seeded into a four chamber tissue culture treated glass slides. When the cells were 30% confluent, PLGA/pSi microspheres containing 65 000 pSi particles were added into each chamber. 65 000 pSi particles were used as control. After 0, 24, 48, and 120 h incubation, cells were washed with PBS and fixed with 4% paraformaldehyde (PFA) for 10 min at room temperature. PFA was removed and washed twice with PBS. Cells were permeabilized. with 0.1% Triton X for 10 min, and then blocked with BSA (1%) in PBS for 30 min at room temperature. Triton X was removed, and cells were incubated with Alexa Fluor 555 conjugated phalloidin in BSA (1%) in PBS for 30 min. Cells were washed and incubated with DRAQ5 for 1 h. DRAQ5 was removed and prolong gold was added on the slides to mount the sample.

In Vitro Cellular Uptake of FITC-BSA: 40 000 HUVEC were seeded and cultured on a glass cover slip in a 12 well plate with 500 million PLGA/pSi microspheres loaded with FITC-BSA in a transwell on top of the cells or 0.1 mg/mL of BSA initially added to the media for 1 hour. The media were changed every 3 days. Cellular uptake of FITC-BSA released from the PLGA/pSi microspheres was observed by confocal microscopy staining cells with fluorescent phalloidin (actin filaments) and DRAQ5 (nuclei) after fixation (10% formaldehyde).

Confocal Microscopy Analysis: Detection of the FITC-BSA loaded pSi particles was based on auto-fluorescence using 488 excitation laser and the cells were analyzed by using 561 and 632 excitation laser for phalloidin and DRAQ5 respectively. Images were acquired using a Leica MD 6000 upright confocal microscope equipped with a 63× oil immersion objective.

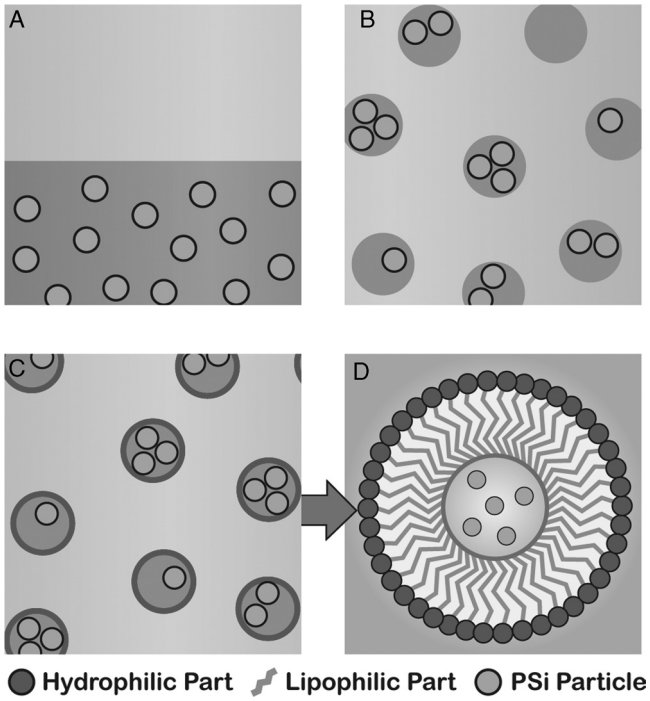

Scheme 1. The schematic diagram of PLGA/pSi microspheres fabrication through the S/O/W emulsion method. A) PLGA/pSi suspension was poured into water phase. B) The suspension was emulsified in the water phase. C) Surfactants were added to stabilize the structures. D) Cartoon depicting the final composition of a PLGA/pSi microsphere (components not in scale).

Supporting Information

Supporting Information is available from the Wiley Online Library or from the author.

Acknowledgements

We thank the Stem Cell Center of Institute of Molecular Medicine, University of Texas Health Science Center at Houston, especially Daniel Blashki for the kind provision of bone stromal stem cells. Thanks Dr. Zhengmei Mao for the help with confocal laser spectroscopy. We thank the US ARMY RDECOM ACQ CTR through the grant W911NF-09-1-0044 (BioNanoScaffolds (BNS) for Post-Traumatic for supporting these studies. We are grateful for the exceptional assistance of Matthew

Landry in the preparation of the images of this manuscript and Song Kim for her editorial comments.

Received: February 21, 2011
Revised: June 9, 2011
Published online: October 19, 2011

[1] L. T. Canham, *Adv. Mater.* **1995**, *7*, 1033.
[2] S. McInnes, N. H. Voelcker, *Future Med. Chem.* **2009**, *1*, 1051.
[3] S. J. P. McInnes, H. Thissen, N. R. Choudhury, N. H. Voelcker, *J. Colloid Interface Sci.* **2009**, *332*, 336.
[4] P. Mukherjee, M. A. Whitehead, R. A. Senter, D. Fan, J. L. Coffer, L. T. Canham, *Biomed. Microdevices* **2006**, *8*, 9.
[5] A. H. Mayne, S. C. Bayliss, P. Barr, M. Tobin, L. D. Buckberry, *Phys. Status Solidi A* **2000**, *182*, 505.
[6] M. A. Whitehead, D. Fan, P. Mukherjee, G. R. Akkaraju, L. T. Canham, J. L. Coffer, *Tissue Eng. A* **2008**, *14*, 195.
[7] M. A. Whitehead, D. Fan, G. R. Akkaraju, L. T. Canham, J. L. Coffer, *J. Biomed. Mater. Res. Part A* **2007**, *83A*, 225.
[8] J. L. Coffer, M. A. Whitehead, D. K. Nagesha, P. Mukherjee, G. Akkaraju, M. Totolici, R. S. Saffie, L. T. Canham, *Phys. Status Solidi A* **2005**, *202*, 1451.
[9] L. T. Canham, *Nanotechnology.* **2007**, *18*, 185704.
[10] F. J. Martin, K. Melnik, T. West, J. Shapiro, M. Cohen, A. A. Boiarski, M. Ferrari, *Drugs R&D* **2005**, *6*, 71.
[11] G. A. Soon-Whatt, C. A. Yaw-Fui, L. R. Houa-Gong, L. Te-Neng, Y. S. Wing-Kwong, C. May, S. Somanesan, L. S. Li-Er, N. D. Chee-Eng, L. Beng-Choo, C. Stephen, C. Pierce Kah-Hoe, *Int. J. Radiat. Oncology. Biol. Phys* **2007**, *67*, 786.
[12] E. J. Anglin, M. P. Schwartz, V. P. Ng, L. A. Perelman, M. J. Sailor, *Langmuir* **2004**, *20*, 11264.
[13] A. B. Foraker, R. J. Walczak, M. H. Cohen, T. A. Boiarski, C. F. Grove, P. W. Swaan, *Pharm. Res.* **2003**, *20*, 110.
[14] C. A. Prestidge, T. J. Barnes, A. Mierczynska-Vasilev, W. Skinner, F. Peddie, C. Barnett, *Phys. Status Solidi A* **2007**, *204*, 3361.
[15] L. Vaccari, D. Canton, N. Zaffaroni, R. Villa, M. Tormen, E. di Fabrizio, *Microelectron. Eng.* **2006**, *83*, 1598.
[16] R. E. Serda, S. Ferrati, B. Godin, E. Tasciotti, X. Liu, M. Ferrari, *Nanoscale* **2009**, *1*, 250.
[17] E. Tasciotti, B. Godin, J. O. Martinez, C. Chiappini, R. Bhavane, X. Liu, M. Ferrari, *Mol. Imaging* **2011**, *10*, 56.
[18] E. Tasciotti, X. Liu, R. Bhavane, K. Plant, A. D. Leonard, B. K. Price, M. M. C. Cheng, P. Decuzzi, J. M. Tour, F. Robertson, M. Ferrari, *Nat. Nanotechnol.* **2008**, *3*, 151.
[19] J. S. Ananta, B. Godin, R. Sethi, L. Moriggi, X. Liu, R. E. Serda, R. Krishnamurthy, R. Muthupillai, R. D. Bolskar, L. Helm, M. Ferrari, L. J. Wilson, P. Decuzzi, *Nat. Nanotechnol.* **2010**, *5*, 815.
[20] C. Chiappini, E. Tasciotti, J. R. Fakhoury, D. Fine, L. Pullan, Y. Wang, L. Fu, X. Liu, M. Ferrari, *ChemPhysChem* **2010**, *11*, 1029.
[21] P. Decuzzi, B. Godin, T. Tanaka, S. Y. Lee, C. Chiappini, X. Liu, M. Ferrari, *J. Controlled Release* **2010**, *141*, 320.
[22] R. E. Serda, A. Mack, M. Pulikkathara, A. M. Zaske, C. Chiappini, J. R. Fakhoury, D. Webb, B. Godin, J. L. Conyers, X. Liu, J. A. Bankson, M. Ferrari, *Small* **2010**, *6*, 1.
[23] J. H. Park, L. Gu, G. von Maltzahn, E. Ruoslahti, S. N. Bhatia, M. J. Sailor, *Nat. Mater.* **2009**, *8*, 331.
[24] T. Tanaka, L. S. Mangala, P. E. Vivas-Mejia, R. Nieves-Alicea, A. P. Mann, E. Mora, H.-D. Han, M. M. K. Shahzad, X. Liu, R. Bhavane, J. Gu, J. R. Fakhoury, C. Chiappini, C. Lu, K. Matsuo, B. Godin, R. L. Stone, A. M. Nick, G. Lopez-Berestein, A. K. Sood, M. Ferrari, *Cancer Res.* **2010**, *70*, 3687.
[25] B. H. Woo, G. Jiang, Y. W. Jo, P. P. DeLuca, *Pharm. Res.* **2001**, *18*, 1600.
[26] M. van de Weert, W. E. Hennink, W. Jiskoot, *Pharm. Res.* **2000**, *17*, 1159.
[27] J. M. Chan, L. Zhang, K. P. Yuet, G. Liao, J. W. Rhee, R. Langer, O. C. Farokhzad, *Biomaterials* **2009**, *30*, 1627.
[28] D. M. K. Jensen, D. Cun, M. J. Maltesen, S. Frokjaer, H. M. Nielsen, C. Foged, *J. Controlled Release* **2010**, *142*, 138.
[29] B. C. Tang, M. Dawson, S. K. Lai, Y.-Y. Wang, J. S. Suk, M. Yang, P. Zeitlin, M. P. Boyle, J. Fu, J. Hanes, *Proc. Natl. Acad. Sci. USA* **2009**, *106*, 19268.
[30] W. J. E. M. Habraken, J. G. C. Wolke, A. G. Mikos, J. A. Jansen, *J. Biomater. Sci., Polym. Ed.* **2008**, *19*, 1171.
[31] W. Linhart, F. Peters, W. Lehmann, K. Schwarz, A. F. Schilling, M. Amling, J. M. Rueger, M. Epple, *J. Biomed. Mater. Res.* **2001**, *54*, 162.
[32] V. P. Torchilin, *Adv. Drug Delivery Rev.* **2006**, *58*, 1532.
[33] J. Salonen, A. M. Kaukonen, J. Hirvonen, V. Lehto, *J. Pharm. Sci.* **2008**, *97*, 632.
[34] D. Fan, G. R. Akkaraju, L. T. Canham, J. L. Coffer, *Nanoscale* **2011**, *3*, 354.
[35] J. Lee, S. Lee, S. Yu, J. Park, J. Choi, J. Kim, *Surf. Coat. Technol.* **2008**, *20*, 5757.
[36] D. C. J. Eisinger, D. Clairet, *Magnes. Res.* **1993**, *6*, 247.
[37] D. M. Reffitt, N. Ogston, R. Jugdaohsingh, H. F. J. Cheung, B. A. J. Evans, R. P. H. Thompson, J. J. Powell, G. N. Hampson, *Bone* **2003**, *32*, 127.
[38] B. Godin, J. Gu, R. E. Serda, R. Bhavane, E. Tasciotti, C. Chiappini, X. Liu, T. Tanaka, P. Decuzzi, M. Ferrari, *J. Biomed. Mater. Res. A* **2010**, *15*, 1236.
[39] S. B. Hartono, S. Z. Qiao, J. Liu, K. Jack, B. P. Ladewig, Z. Hao, G. Q. Max Lu, *J. Phys. Chem. C* **2010**, *114*, 8353.
[40] X. Huang, X. Meng, F. Tang, L. Li, D. Chen, H. Liu, Y. Zhang, J. Ren, *Nanotechnology* **2008**, *19*, 5101.
[41] A. J. Milligan, F. M. M. Morel, *Science* **2002**, *297*, 1848.
[42] M. S. Bawa, V. S. Simpson, P. A. Miller, F. L. Allen, G. L. Etheridge, K. J. L'anglois, M. H. Grimes, *United States Patent 6028006*, **2000**.
[43] M. Das, T. Miyakawa, C. F. Fox, R. M. Pruss, A. Aharonov, H. R. Herschman, *Proc. Natl. Acad. Sci. USA* **1977**, *74*, 2790.
[44] Y. Xiao, S. P. Forry, X. Gao, R. D. Holbrook, W. G. Telford, A. Tona, *J. Nanobiotechnol.* **2010**, *8*, 13.
[45] G. Sharma, D. T. Valenta, Y. Altman, S. Harvey, H. Xie, S. Mitragotri, J. W. Smith, *J. Controlled Release* **2010**, *147*, 408.
[46] Y. J. Ma, H. C. Gu, *J. Mater. Sci. Mater. Med.* **2007**, *18*, 2145.
[47] R. A. Gemeinhart, D. Luo, W. M. Saltzman, *Biotechnol. Prog.* **2005**, *21*, 532.
[48] H. A. Lucero, E. Kintsurashvili, M. E. Marketou, H. Gavras, *J. Biol. Chem.* **2010**, *285*, 5555.
[49] X. Huang, X. Meng, F. Tang, L. Li, D. Chen, H. Liu, Y. Zhang, J. Ren, *Nanotechnology* **2008**, *19*, 5101.
[50] R. N. Jorissen, F. Walker, N. Pouliot, T. P. J. Garrett, C. W. Ward, A. W. Burgess, *Exp. Cell Res.* **2003**, *284*, 31.
[51] G. Carpenter, S. Cohen, *J. Cell. Biol.* **1976**, *71*, 159.
[52] L. Beguinot, R. M. Lyall, M. C. Willingham, I. Pastan, *Proc. Natl. Acad. Sci. USA* **1984**, *81*, 2384.
[53] A. Sorkin, C. M. Waters, *Bioessays* **1993**, *15*, 375.
[54] A. Raz, C. Bucana, W. E. Fogler, G. Poste, I. J. Fidler, *Cancer Res.* **1981**, *41*, 487.
[55] C. Reis e Sousa, P. D. Stahl, J. M. Austyn, *J. Exp. Med.* **1993**, *178*, 509.
[56] R. Heumann, M. Schwab, R. Merkl, H. Thoenen, *J. Neuroscience* **1984**, *4*, 3039.
[57] M. L. Ho, Y. C. Fu, G. J. Wang, H. T. Chen, J. K. Chang, T. H. Tsai, C. K. Wang, *J. Controlled Release* **2008**, *128*, 142.